Crude oil sorbent based on cellulose nanofibrils-methacrylate grafted copolymers

Natalya Grechishcheva, *Irina* Grishina, *Alexandra* Kuchierskaya, *Andrey* Panchenko, *Dmitry* Kopitsyn, *Valentina* Lyubimenko*, *Andrey* Novikov, and *Vladimir* Vinokurov

Gubkin University, Department of Physical and Colloidal Chemistry, 119991 Moscow, Russia

Abstract. Hydrophobic composites of cellulose nanofibrils (CNF) with acrylic polymers are obtained by methyl methacrylate (MMA) and butyl methacrylate (BMA) polymerization in Pickering emulsion, stabilized with cellulose nanofibrils. Successful modification of CNF surface by grafting MMA or BMA was confirmed by infrared spectroscopy, gel permeation chromatography, and scanning electron microscopy. The obtained composites were also characterized by simultaneous thermal analysis and wetting contact angle measurement. Composites based on CNF exhibit good thermal and oil sorption properties.

1 Introduction

Nowadays, the negative impact of oil pollution on the environment is becoming more significant due to increased oil spill accidents [1]. Most of these accidents occur along with transportation with pipelines and ground transport, operations at offshore oil terminals, disasters on oil tankers and offshore drilling platforms, discharge of industry, and daily wastewater containing petroleum products. These accidents can lead to the death of marine animals, birds, and fish. Besides, the polycyclic aromatic hydrocarbons present in petroleum affect many biological processes and act as potential cell mutagens and carcinogens [2]. Oil spills damage not only wildlife but also coastal settlements economics. Thus, now it is essential to develop effective methods to eliminate the consequences of such accidents.

To date, there are three major classes of oil spill cleanup methods: physical, chemical, and biological. Chemical methods, including chemical dispersants and direct combustion, can cause secondary pollution, while biological methods are expensive, making sorption one of the highly recommended techniques for oil spill treatment. Using oil sorbents is cost-effective, easy to operate, and eco-friendly [3]. However, most of the existing sorbents do not provide high adsorption efficiency and require complex recovery procedures. Due to their porous structure and large specific surface area, three-dimensional (3D) aerogels are among the most promising oil spill cleanup materials [4]. Synthetic polymeric and carbon aerogels demonstrate very high absorption capacity and good recyclability, but sophisticated preparation procedures, high cost, and environmental damage significantly complicate their usage.

* Corresponding author: ljubimenko@mail.ru

In contrast, oil spill cleanup materials from natural fibers combine simplicity of preparation, low cost, and good biodegradability [5]. Fibrous materials are easy to store and handle, and the high tensile strength of cellulose provides good mechanical properties of these materials [6, 7].

Cellulose nanofibrils (CNFs) are especially suitable for producing cellulose-based composite materials. CNFs can be produced from technical-grade softwood cellulose with a yield of more than 80% [8]. CNFs form the structural support for the functional component of the composite material, even at low cellulose content [9]. Besides, CNFs are biocompatible and biodegradable, which enables a broad spectrum of applications: oil-absorbing [10-13], ion-exchange [14], packaging [15], and antibacterial [16] materials, to name a few.

Mainstream methods for producing cellulose-based composites are solvent casting and co-extrusion. However, they require drying, milling, and solvent exchange, which increase the cost of composites.

As an alternative method, monomers could be graft-polymerized onto the cellulose surface, thus providing high surface area and hydrophobicity [17]. Radical polymerization of vinyl-substituted substances is widely employed for such grafting. In addition to free-radical initiators, cellulose surface could enhance the polymerization *via* the generation of surface-bound radicals (surface-initiated atom transfer radical polymerization, SI-ATRP) [18].

In this study, we present the preparation of CNFs-based materials by the graft polymerization of methyl methacrylate and butyl methacrylate onto cellulose nanofibrils, their characterization by various physic-chemical methods, and the estimation of their crude oil absorption properties. The preparation of materials involves technical-grade cellulose and cheap industrial chemicals, making the obtained composites available for large-scale production.

2 Materials and methods

2.1 Materials

Sodium dodecyl sulfate (SDS), N,N-dimethylformamide (DMF), methyl methacrylate (MMA), and butyl methacrylate (BMA) were acquired from Sigma-Aldrich (St. Louis, MO, USA). Ammonium persulfate and sulfuric acid were purchased from Chimmed (Moscow, Russia). Deionized water with a resistivity of 18.1 MΩ·cm was prepared with a Simlicity UV system (Millipore, USA).

CNFs were prepared as described elsewhere [8]. Briefly, unbleached technical-grade cellulose pulp was dispersed in water with MSM66110 blender (Bosch, China), mixed with ammonium persulfate and sulfuric acid (1.33 and 2.67 mole/kg in the obtained solution, respectively), and shaken for 4 hours at 180 rpm (Biosan ES20/60, Latvia). The dispersion was filtered, washed with distilled water until pH=6.5, sonicated in distilled water (Branson Scientific S-450, USA), and then homogenized with Ultraturrax T-18 (IKA, Germany). CNFs size was estimated by laser diffraction (Malvern Mastersizer 3000, Malvern, UK) and transmission electron microscopy (Jeol JEM-2100, Japan).

2.2 Methods

2.2.1 Preparattion of cellulose nanofibrils – acrylic polymers composites

A monomer emulsion was prepared by sonication of methyl methacrylate or butyl methacrylate in water (Branson Scientific S-450, USA) in the presence of SDS (0.1%). CNFs dispersion in water (5 wt. %) was stirred (300 rpm, Biosan MSH-300), and monomer

emulsion was added drop by drop in 30 minutes. Then ammonium persulfate was dissolved in the resulted dispersion. Weight ratios of CNFs, monomer, and initiator were (30:70:0.14). The resulting mixture was heated to 80 °C for 5 hours while stirring and cooled to room temperature. The composite was vacuum-filtered on the Schott funnel with a 16-µm sintered-glass filter and washed three times with distilled water to remove ammonium salts and soluble by-products. Then the composite was dried at 70 °C for 12 hours, obtaining the CNF-MMA and CNF-BMA samples.

2.2.2 Characterization of composites

The efficiency and completeness of the polymerization process were monitored by infrared spectroscopy (IR), gel permeation chromatography (GPC), and scanning electron microscopy (SEM). The obtained composites were also characterized by simultaneous thermal analysis (STA) and contact angle (CA).

Contact angle measurements were performed using a DSA100 Contact Angle Measuring System (Krüss, Hamburg, Germany) by the sessile drop method. For these measurements tablets from boric acid with a layer of composites samples on the surface were prepared using laboratory hydraulic press LHP-25 (Lab Tools, Russia). Contact angle was determined under the layer of cyclohexane in the cuvette held at the temperature of 20 °C using the circulation water bath MPC-E (Huber, Offenburg, Germany).

The thermal behavior of the obtained composites was studied using the STA 449F5 system (Netzsch, Germany) with the temperature programming from 303 K to 673 K at 10 K/min.

Scanning electron micrographs were registered using the dual-beam JIB-4501 system (Jeol, Tokyo, Japan) at the accelerating voltage of 10 kV.

The IR spectra of the studied samples in the form of thin films or compressed tablets were recorded on a Nicolet iS10 IR Fourier spectrometer (Thermo Scientific, USA) using Smart iTR™ Attenuated Total Reflectance (ATR) Sampling Accessory with a Ge crystal in the mid-infrared range of 4000–400 cm^{-1} with a spectral resolution of 8 cm^{-1}. The sample was placed on a crystal and fixed with a clamping element. The accumulation time was 14 s for each spectrum. The data were registered and processed using the OMNIC Thermo Scientific software.

For obtaining molecular weight distribution samples of CNF-MMA and CNF-BMA composites were dissolved in DMF. GPC was performed using the Agilent 1260MDS system (Agilent, USA) with two series-connected Polargel M 30×7.5 columns in DMF solvent at an eluent flow of 1 mL/min. The volume of the injected sample was 100 µL. The samples were filtered immediately before entering into the chromatographic column using 0.2 µm PTFE syringe filters. Based on the signal of the refractometric and viscometric detectors, the molecular weight distribution of the samples was reconstructed using the universal calibration curve according to the Mark-Kuhn-Houwink equation. Standard samples of methyl methacrylate with a known molecular weight were used to construct the calibration curve.

2.2.3 Oil absorbtion tests

The sorption properties of the obtained samples were evaluated according to the following method. Squares of copper mesh with an area of 25 cm^2 were cut out, and fasteners made of copper wire were placed in the corners. The resulting copper mesh baskets were weighed on the aluminum foil plates with the analytical balances.

First, a blank test was performed. The copper mesh baskets ($\underline{m}_c$) prepared for the test were weighed on an analytical balance, immersed in oil or petroleum products, and kept there for

15-45 minutes. Then the copper mesh baskets were removed from the oil, allowed to drain the oil excess, and weighed on the aluminum foil plate. The measurement was repeated three times. Each time the copper mesh baskets were washed with gasoline, dried, and the aluminum foil plate was replaced.

Next, the sorption capacity of the obtained CNF/MMA and CNF/BMA samples was measured. A layer of pre-weighed sorbent (m_1) was placed on a clean copper mesh basket. The basket with the sorbent was immersed in oil or petroleum product and held there for 15-45 minutes, and then was removed and allowed to drain the oil excess. After the oil completely stopped dripping from the mesh, the mesh was carefully removed from the structure, and the sorbent with the absorbed oil was removed for further weighing. The copper mesh with the spent sorbent was weighed on the aluminum foil plate (m_2).

The sorption capacity of the sorbents (C, g/g) was then calculated according to the formula:

$$C = \frac{m_2 - m_C - m_1}{m_1}, \quad (1)$$

m_1 – weight of pure sorbent, m_c – weight of the copper mesh basket, m_2 - copper mesh with the sorbent and absorbed oil.

3 Results and discussion

In order to compare the IR spectra of the polymers obtained on CNF and similar spectra of pure polymers, the latter were obtained under the conditions of Pickering-emulsion polymerization, where halloysite-based aluminosilicate nanotubes were used as the colloid phase in the same concentrations as CNF.

Fig. 1 shows the IR spectra of the original unmodified CNF and MMA/BMA grafted CNF.

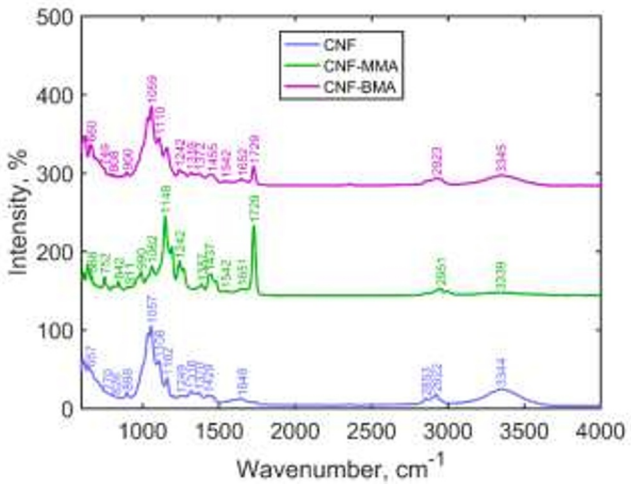

Fig. 1. IR spectra of the pristine CNF and grafted MMA/BMA CNF.

The IR spectrum of the unmodified CNF includes the wide band in the region of 3000-3600 cm^{-1} that is related to OH groups having hydrogen bonds. The band at 2850-2951 cm^{-1} is attributed to stretch vibrations of C-H groups; the band at 1600-1700 cm^{-1} indicates the OH presence of adsorbed water; the band at 1300-1455 cm^{-1} is caused by vibrations of CH

and CH_2 groups; the band at 1162-1000 cm^{-1} is ascribed to C–O–C asymmetric stretching and C–C, C–OH, C–H vibrations; the peak at 898-900 cm^{-1} is related to C–O–C, C–C–O and C–C–H deformation and stretching.

In the spectra of MMA/BMA grafted CNF the wide band in the region of 3000-3600 cm^{-1} related to OH groups was decreased in great extent. (Fig.1). The MMA/BMA modified CNF showed a strong band at 1729 cm^{-1} which was attributed to C=O (carbonyl group of esters stretching) in the PMMA/PBMA chains of the polymer backbone. Another peak at 842 cm^{-1} is exhibited due to the deformation vibration of C–O–C single bonds. Also, CNF and its MMA/BMA grafted copolymers displayed absorption bands at 1429, 1437, 1455 cm^{-1} of CH_2 bending and band at1162 cm^{-1} of asymmetric C–O–C-stretching vibrations. The chemical bonding of MMA or BMA polymers to the cellulose backbone decreases its hydrophilicity and increases hydrophobicity which shows the possibility of its application in the oil absorption.

The hydrophobic properties of grafted CNF samples are confirmed by measurements of the wetting angle formed by a water droplet with the surface of these materials. The wetting angle of the water droplet on unmodified CNF, as well as MMA and BMA grafted CNF is shown in Fig. 2 (*a*, *b*, *c*).

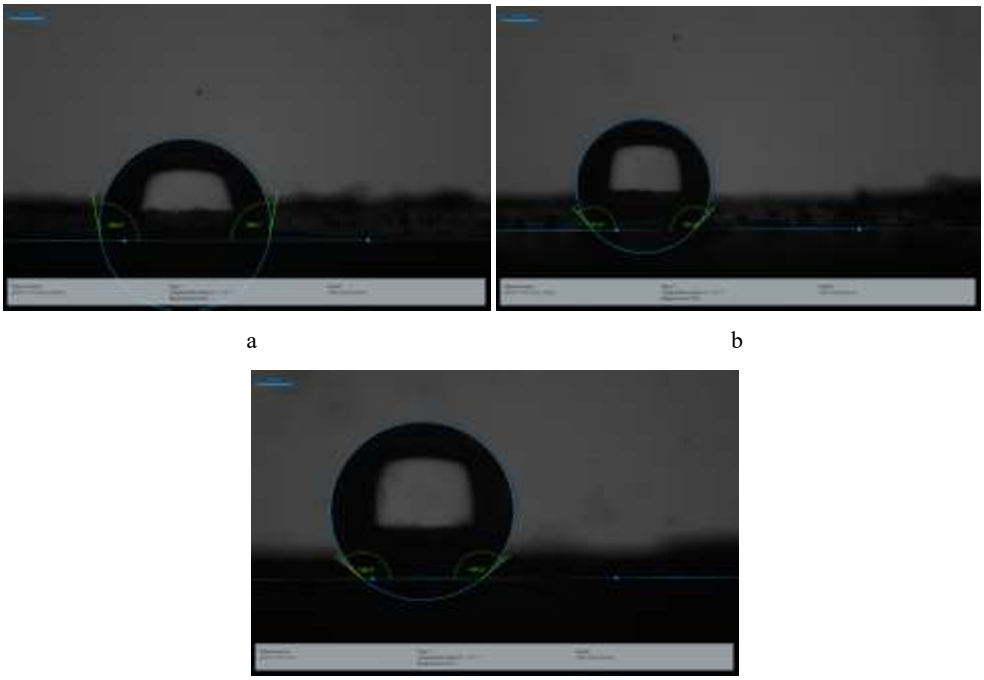

a b

c

Fig. 2. Contact angle of the water droplet on: *a*) CNF; *b*) MMA grafted CNF; *c*) BMA grafted CNF.

The wetting angle of the water droplet on the pure CNF is 100.2° (Fig. 2, *a*). After grafting the MMA to the CNF surface the value of the wetting angle is raised to 131.4° (Fig. 2, *b*). Grafting BMA to the surface of the CNF causes an increase in the wetting angle to 140.3° (Fig. 2, *c*). The experimental data indicate higher hydrophobicity of the CNF-BMA surface compared to the CNF-MMA sample.

SEM micrographs in Fig. 3(*a*, *b*) shows the surface microstructure of the CNF-MMA and CNF-BMA samples. CNF fibers modified by grafting have both hydrophobic properties and due to roughness, a larger specific surface area (Fig. 3). These properties make it possible to

use modified CNF as an effective sorbent for oil spills recovery and water purification from oil pollution.

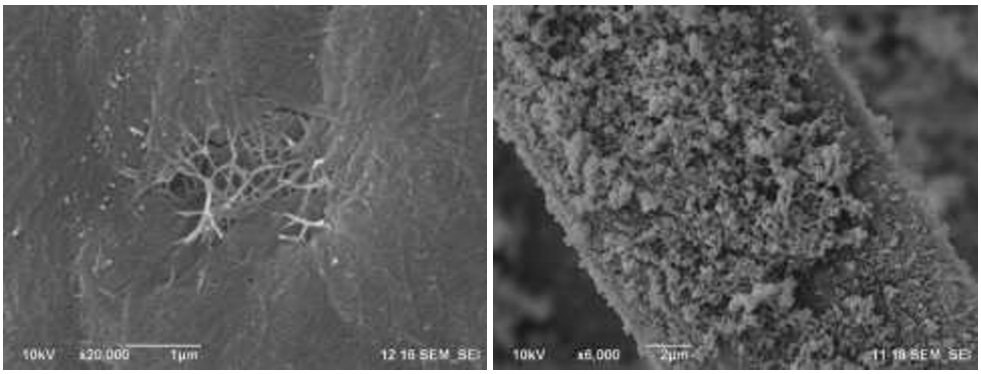

a b

Fig. 3. SEM micrographs: *a*) CNF-MMA sample; *b*) CNF-BMA sample.

The estimated weight average molecular weight of CNF copolymers with MMA/BMA (M_w) was approximately $1.5 \cdot 10^6$ g/mol and $1.8 \cdot 10^6$ g/mol, respectively.

The results of STA and DSC analysis of the pristine CNF, CNF-MMA and CNF-BMA composites are presented in Fig.4 (*a*, *b*).

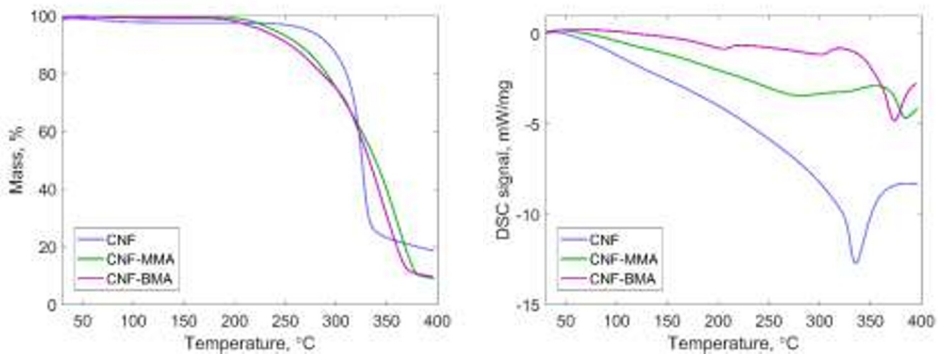

a b

Fig. 4. The data of STA (*a*) and DSC (*b*) analysis.

From Fig. 4*a* it follows that the first stage of unmodified CNF thermal degradation occurs between 50 and 200 °C, in which dehydration takes place with the weight loss of 2%. The second degradation stage of CNF ranges between 200 and 300 °C which resulted in 5 % weight loss, and the third stage ranges between 300 and 400 °C, which is responsible for the decomposition of cellulose chains. The overall weight loss of CNF was 81 %.

The first stage of MMA/BMA grafted CNF dehydration takes place in the temperature range between 50 and 200 °C, the weight loss is near 1 %. The percentage weight loss of MMA/BMA grafted CNF at the second degradation stage (200-300 °C) was 70 %, at the third stage (300-400 °C) it was and overall weight loss results in 90%. The third degradation stage (300–400 °C) of MMA/BMA grafted CNF consists of thermal decomposition of polyMMA/BMA chains bonded with the CNF fibres backbone and decomposition of cellulosic compounds.

The data of DSC (Fig. 4*b*, Table 1) showed the peak of CNF decomposition at 335,5 °C and three decomposition peaks on the curves for CNF-MMA (205.4, 301.3, and 373.3 °C)

and CNF-BMA (for MMA grafted CNF; for BMA grafted CNF 281.2, 316.1, 384.9 °C). The results of the DSC allow us to conclude that the CNF grafted with MMA is the most stable compared to pure and BMA grafted CNF.

Table 1 summarizes data on the ability to sorb oil, wettability and thermal properties of sorbents based on cellulose nanofibrils.

Table 1. Oil sorption capacity, wettability and thermal stability of the tested materials.

Sample	Crude oil sorption, g/g								Initial wetting angle, °	Thermal analysis			
	Oil, ρ=0,88 g/cm³					Oil, ρ=0,84 g/cm³				Residual mass at 400 °C, %	DSC peaks,°C		
CNF	12.57	14.17	14.35	-	-	29.2	29.7	29.5	100.2	19	-	-	335.5
CNF:BMA 30:70	1.34	1.48	0.15	-	-	3.89	2	3.14	140.3	~10	205.4	301.3	373.7
CNF:MMA 30:70	9.75	9.5	8.83	10.8	7.9	13.05	12.56	12.36	131.4	~10	281.2	316.1	384.9

From the Table 1 data it follows that the average sorption capacity of CNF is 13.7 g/g for oil with the density of 0.88 g/cm^3 and 29.5 g/g for oil with the density of 0.84 g/cm^3. For grafted BMA CNF the average sorption capacity is 0.99 and 3.01 g/g for these oils, accordingly. The MMA grafted CNF exhibits a sorption capacity of 9.36 g/g for the oil having density of 0.88 g/cm^3 and 12.66 g/g for the oil having density of 0.84 g/cm^3.

4 Conclusions

Hydrophobic composite material based on CNF is obtained by grafting of MMA/BMA onto surface of cellulose in a Pickering emulsion. Polymerization of acrylic monomers in the Pickering emulsion stabilized by CNF proceeds with high yields (86-90%) with the formation of high-molecular polymers with M_W $1.5 \cdot 10^6$ -$1.8 \cdot 10^6$ g/mol.

The average particle size of the resulting emulsion is 150-200 nm, as evidenced by the data of scanning electron microscopy of the resulting polymers.

The sorption capacity for oil (ρ=0,84 g/cm^3) decreases in a row CNF>MMA grafted CNF>BMA grafted CNF and is equal to 29.5, 12.66, 3.01 g/g, respectively.

Despite the decrease in the sorption capacity of CNF-based composites compared to the sorption capacity of the starting material, their use is advisable due to the reduction in the cost of obtaining sorbents (lower cost of acrylic monomers compared to CNF, ease of separation and drying of polymer composites), higher resistance to water and improved thermal and mechanical properties.

The obtained composites may be of interest both from the point of view of obtaining sorbents for the oil spill recovery, water purification from petroleum products, and from the point of view of obtaining biphilic matrices for bactericidal coatings, electrically conductive membranes, carriers of hydrophilic and oleophilic drugs.

References

1. J. Chen, W. Zhang, Zh. Wan; S. Li, T. Huang, Y. Fei, J. Clean. Prod. **227**, 20 (2019)
2. H. I. Abdel-Shafy, M. S. M. Mansour, EGYJP **25**, 1 (2016)
3. J. Saleem, M. A. Riaz, M. K., J. Hazard. **341**, 424-437 (2018)

4. W.-J. Yang, A. Ch. Y. Yuen, A. Li, B. Lin, T. B. Y. Chen, W. Yang, H.-D. Lu,, G. H. Yeoh, Cellulose **11**, 6449-6476 (2019)
5. F. Chu, Z Xu, X. Mu, W. Cai, X. Zhou, W. Hu, L. Song, Cellulose **27**, 3485–3499 (2020)
6. R. Hollertz, V. L. Durán, P. A. Larsson et al., Cellulose **24**, 3883–3899 (2017)
7. Y. Wu, Q. Tang, F. Yang et al., Cellulose **26**, 3193–3204 (2019)
8. A. Novikov, B. M. Anikushin, D. Petrova et al., Chem Technol Fuels Oils **54**, 564–568 (2018)
9. V. Vinokurov, A. Novikov, V. Rodnova, B. Anikushin, M. Kotelev, E. Ivanov, Yu. Lvov, Polymers **11**, 5, (2019)
10. Yu. Liu, T. Shi, T. Zhang, D. Yuan, Y. Peng, F. Qiu, Cellulose **26**, 9 (2019)
11. Y. Zhao, K. Zhong, W. Liu, Sh. Cui, Y. Zhong, Sh. Jiang, Cellulose **27**, 13 (2020)
12. L. Yang, B. Bai, Ch. Ding, H. Wang, Y, Suo, RSC Adv. **6**, 12, (2016)
13. J. Jiang, Q. Zhang, X. Zhan, F. Chen, ACS Sustain. Chem. Eng. **5**, 11 (2017)
14. S. Eun, H.-J. Hong, H. Kim, H. S. Jeong, S. Kim, J. Jung, J. Ryu, Carbohydr. Polym. **235**, 115984 (2020)
15. W. Li, S. Wang, W. Wang, Ch, Qin, M, Wu, Cellulose **26**, 3271–3284 (2019)
16. H. Durand, P. Jaouen, E. Faure, C. Sillard, N. Belgacem, E. Zeno, J. Bras, Cellulose **27**, 7037–7052 (2020)
17. H. Hoshina, J. Chen, H. Amada, N. Seko, Polymers **12**, 2656 (2020)
18. D. Cheng, P. Wei, L. Zhang, J. Cai, RSC Adv. **8**, 48 (2018)